energies

MDPI

Article

Behavior of XLPE for HVDC Cables under Thermo-Electrical Stress: Experimental Study and Ageing Kinetics Proposal

Hanen Yahyaoui [1,*], Jerome Castellon [1], Serge Agnel [1], Aurelien Hascoat [2], Wilfried Frelin [2], Christophe Moreau [2], Pierre Hondaa [3], Dominique le Roux [4], Virginie Eriksson [4] and Carl Johan Andersson [4]

1 Institut d'Electronique et des Systèmes, Université Montpellier, CNRS, 34090 Montpellier, France; jerome.castellon@ies.univ-montp2.fr (J.C.); serge.agnel@ies.univ-montp2.fr (S.A.)
2 EDF R&D, 77250 Les Renardières, France; aurelien.hascoat@edf.fr (A.H.); wilfried.frelin@edf.fr (W.F.); christophe.moreau@edf.fr (C.M.)
3 RTE, 92919 Paris la Défense, France; pierre.hondaa@rte-france.com
4 BOREALIS, 444 86 Stenungsund, Sweden; Dominique.LeRoux@borealisgroup.com (D.l.R.); Virginie.Eriksson@borealisgroup.com (V.E.); CarlJohan.Andersson@borealisgroup.com (C.J.A.)
* Correspondence: hanen.yahyaoui@gmail.com

Abstract: The present work deals with the study of the electrical behavior of cross-linked polyethylene (XLPE) used for HVDC cable insulation. The aim is to better understand the influences of electrical and thermal stresses on the insulating material in order to provide useful information for designing HVDC cables. This study was carried out on Rogowski samples made of XLPE insulation with semiconductive electrodes, aged for more than 3 years (1220 days) at three different temperatures (70, 80 and 90 °C) under two DC electric fields (30 and 60 kV/mm). Dielectric loss factor, volume resistivity and space charge accumulation were measured. Results are analyzed and cross-correlated, in order to propose possible ageing kinetics.

Keywords: HVDC; XLPE cable; ageing; space charge; electric field; dielectric spectroscopy

check for updates

Citation: Yahyaoui, H.; Castellon, J.; Agnel, S.; Hascoat, A.; Frelin, W.; Moreau, C.; Hondaa, P.; Roux, D.l.; Eriksson, V.; Andersson, C.J. Behavior of XLPE for HVDC Cables under Thermo-Electrical Stress: Experimental Study and Ageing Kinetics Proposal. *Energies* **2021**, *14*, 7344. https://doi.org/10.3390/en14217344

Academic Editor: Andrea Mariscotti

Received: 31 August 2021
Accepted: 30 October 2021
Published: 4 November 2021

Publisher's Note: MDPI stays neutral with regard to jurisdictional claims in published maps and institutional affiliations.

Copyright: © 2021 by the authors. Licensee MDPI, Basel, Switzerland. This article is an open access article distributed under the terms and conditions of the Creative Commons Attribution (CC BY) license (https://creativecommons.org/licenses/by/4.0/).

1. Introduction

Cross-linked polyethylene (XLPE) is widely used as an electrical insulation material in AC extruded power cables and has a track record of more than 40 years. In the context of a growing interest and demand in high voltage direct current (HVDC) transmission, and because of its high dielectric strength and electrical resistivity, combined with its good mechanical and thermal properties [1], XLPE is also used in extruded HVDC cables. However, the effects of electrical stress on insulating materials under HVAC and HVDC are very different. In fact, the field distribution in DC is determined by the electric resistivity of the insulation, which depends on the temperature and on the applied field [2]. Different empirical formulas have been proposed to describe the variation of DC resistivity of solid insulations with temperature and electric field. An example of such a formula is as follows [3]:

$$\rho_v = \rho_0 \exp(-\alpha T - \beta E) \quad (1)$$

where ρ_0 is the electric resistivity at low electric field and reference temperature, T is the temperature, E is the electric field at the point considered and α and β are the temperature and the electric field coefficients, respectively.

Due to the importance of electrical conduction in insulation materials, especially in HVDC cables, more studies must be conducted on electrical conduction and especially its relationship with ageing.

Under DC conditions, it has been reported that space charge accumulated could generate a residual electric field that can locally overstress the insulation [4,5]. It has been observed that after long periods of polarization under DC conditions, the local electric field of XLPE can be greatly increased [6]. The increased local stress generated by space

charge accumulation is likely to accelerate ageing and may lead to premature electrical breakdown of the insulating material [4,6–9].

It has been demonstrated that space charge injection and accumulation in XLPE insulation is affected by many factors such as electrical and thermal stresses, temperature variations, presence of additives, and peroxide decomposition products, among others [4,8,10–13]. It has been shown, for example, that peroxide decomposition products lead to the formation of heterocharges in XLPE [10–12]. Heterocharges enhance the local electric field, and sometimes it becomes more than three times the initial applied electric field [13].

There are much data available in literature showing that, depending on material, and treatment, the value of the threshold field for space charge accumulation varies considerably. This value was defined between 10 and 20 kV/mm in [14]. An enhancement of local electric field about 100% under an applied DC field between 100 kV/mm was reported after polarity reversal in [12].

These results underline the complexity of space charge behavior and the necessity of measuring space charge in XLPE cable insulations.

The experimental study of space charge effects has been considerably improved by the development of several methods for measuring charge distribution in solid insulation. Among these methods are the Thermal Step Method (TSM) [5,15], the Pulse Electro-Acoustic (PEA) [16], the Pressure Wave Propagation Method [17] and the Laser Induced Pressure Pulse [18]. The TSM was used for the monitoring of the space charge accumulation in this study. This method is based on the diffusion of a thermal wave, which generates temporary local displacements of the space charge. This results on a capacitive current (TSM signal), which depends on the field (and thus electric charge) distribution across the sample. The TSM method allows space charge measurements on plane and cylindrical samples (e.g., cables) [5,15].

As space charge density is dependent on temperature and changes with electrical stress and its application times [2,5,11,15], it is very important to understand the relation between space charge accumulation and XLPE ageing, especially under DC conditions. Published reports have focused on thermal, thermo-oxidative and mechanical ageing [19,20], as well as electrical and water treeing [2]. The effect of polarity reversals on XLPE and water tree retardant when submitted to DC stress for long periods is also investigated [11,12]. Nevertheless, to date, little work has been done on the impact of a combined electrical and thermal stress on dielectric properties of XLPE during long-term ageing tests. An example is the work done by J. Cenes et al. and detailed in [21]. The study concerns the effect of electrothermal and thermal ageing on XLPE model cables for up to 18 months at an average field of 60 kV/mm. Results up to 84 days show that space charge patterns differ considering thermal and electrothermal stress. It was observed that charge density intensifies with ageing time for the thermal cable, but for the electrothermal cable a small positive heterocharge was detected and seemed to increase with ageing time, but remained very low compared to the thermal cable. A decrease of the conductivity was observed. The effect is more important with thermal stress than with electro-thermal stresses.

These results are presented up to 84 days, but long-term results (up to 18 months) are not yet published.

The purpose of this work is to investigate the evolution of dielectric properties of XLPE subjected to electrical and thermal ageing test, in order to assess its suitability for use under a high DC electric field for long durations. The ultimate objective was to identify possible ageing markers that can be used to establish a lifetime model. Several dielectric properties of the material, such as electrical capacitance, loss factor, volume resistivity and space charge accumulation were monitored during more than 3 years of an ageing test. Results are presented and discussed, and an ageing model based on a different hypothesis is proposed.

2. Materials and Methods

2.1. Samples

Rogowski-type samples, provided by Borealis (Figure 1), were made using a conventional HVDC XLPE cable insulation material rated for voltage up to 320 kV, and a semiconductive cross-linkable XLPE commercially available for HVDC applications. The insulation material was first molded by compression at 120 °C in order to form the Rogowski shape. Thereafter, semiconductive plaques were added on both side of the insulation shape and all layers are crosslinked together at 180 °C. In order to reduce the amount of peroxide decomposition products to a very low level, samples were degased for 72 h at 70 °C.

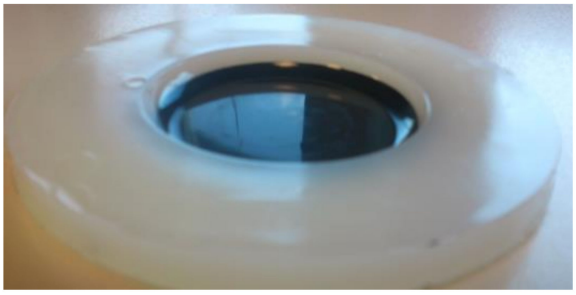


Figure 1. XLPE Rogowski-type sample.

The sample geometry is shown in Figure 2. The dimensions of the active area were 50 mm in diameter with insulation thickness of d = 0.5 or d = 1.0 mm. The sample profile was thicker on the edge than in the center in order to reduce field enhancement at the edges of the electrodes. On each side of the active area, the sample was provided with two semiconductor electrodes with a thickness of about 0.2 mm.

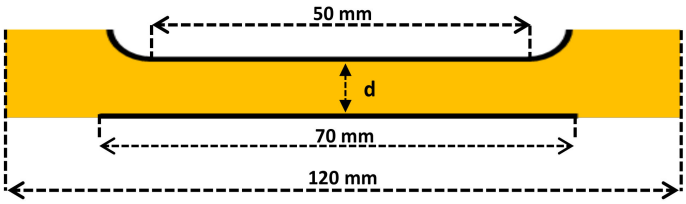


Figure 2. Design of XLPE Rogowski-type sample.

2.2. Experimental Set-Up

2.2.1. Ageing Conditions and Set-Up

As the electric field applied to HVDC cable insulation under service conditions (320 kV) is about 15 kV/mm on average (varying according to the thermal gradient within the insulation, the thickness and the applied voltage), and in order to accelerate ageing, two ageing fields were fixed for this study: 30 and 60 kV/mm.

Ageing was performed at three temperatures (70, 80 and 90 °C). The ageing test was performed in air during for 3 years at the three temperatures.

For each temperature, a thermal regulated oven was used to host 20 samples (10 with d= 0.5 mm and 10 with d = 1 mm). A high DC voltage power supply was used to apply 30 kV to the samples (Figure 3). Thus, 0.5- and 1-mm samples were submitted concomitantly to DC electric fields of 60 and 30 kV/mm, respectively.

Monthly, the samples were removed from the ageing test set-up for capacitance, loss factor, volume resistivity and space charge characterization.

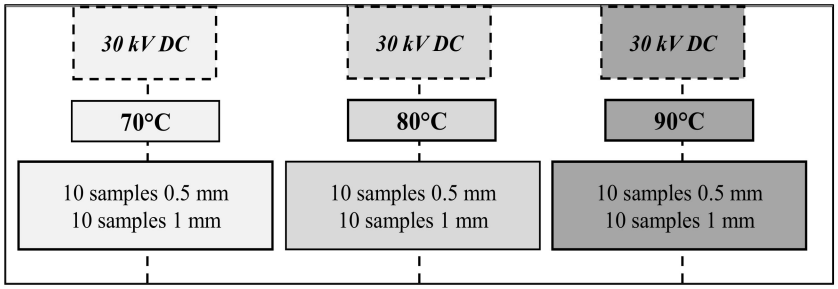


Figure 3. Ageing set-up: summary of the different ageing conditions.

2.2.2. Dielectric Spectroscopy

Dielectric spectra were measured with a specific test cell using a Solartron 1260 frequency analyzer coupled to a Solartron 1296 dielectric interface. Measurements were carried out monthly for 1220 days at room temperature, under an RMS AC voltage of 2 V, at a frequency range of 10^5 to 10^{-1} Hz. In order to obtain statistically representative results, each reported value is the average of four consecutive measurements on the same sample.

2.2.3. Volume Resistivity

The electrical volume resistivity evolution of the material was monitored monthly for 857 days under two electric fields (2 and 30 kV/mm) at 70 °C for all the ageing tests. Quasi-steady state currents were measured after 100 min.

The experimental setup used for the conduction current measurements is shown schematically in Figure 4. The samples were placed in a temperature-regulated oven. A low residual ripple 35 kV HVDC power supply (Fug HCP140-35000) and a Keithley 6517A electrometer were used.

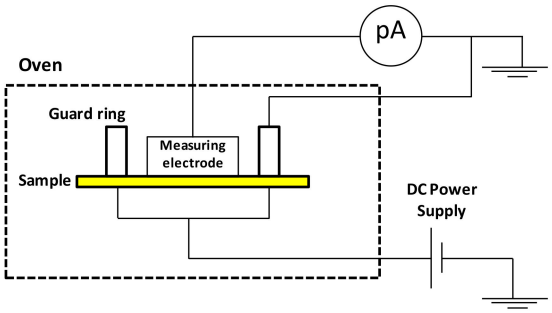


Figure 4. Experimental set-up for conduction current measurements.

The charging currents were recorded for applied voltages of 2 and 30 kV at 70 °C. Quasi-steady state currents were obtained after a transient regime of 100 min. When the stable regime was reached, the electric stress was removed. The samples were then short-circuited until the current came down to a value below the noise level. The value of volume resistivity was then calculated using this conduction current measurement.

2.2.4. Space Charge Measurements

The evolution of space charge accumulated during ageing was monitored monthly for 1220 days (as explained in Figure 3) by using a nondestructive technique: the Thermal Step Method (TSM) [5]. The measurements were made in short-circuit conditions with a thermal step of −30 K (25 °C to −5 °C). To take into account the experimental variations (due to experimental set-up and/or sample heterogeneities), measurements were performed each time on five samples among the ten aged under the same conditions. After measuring the thermal step current, mathematical processing was performed on one sample for each ageing conditions The electric field profile and the space charge density were then obtained.

3. Results

In this section, we present and discuss the main results obtained by electrical volume resistivity, dielectric spectroscopy and space charge measurements.

3.1. Electrical Volume Resistivity

Electrical volume resistivity values measured during ageing conditions under 30 and 60 kV/mm at 70, 80 and 90 °C for 857 days are presented in [22,23]. Electrical volume resistivity did not show any significant evolution as a function of ageing time, for all temperatures and electric fields studied [22]. In this section, we present only results for ageing tests under 30 kV/mm and 60 k V/mm at 90 °C. Values for ageing under 30 kV/mm measured under 2 kV/mm were between 10^{14} Ω × m and 10^{15} Ω × m, whatever the ageing temperature, while those measured under 30 kV/mm were lower than those under 2 kV/mm and are on average of the order of 10^{12} Ω × m and 10^{13} Ω × m. For ageing under 60 kV/mm, electrical volume resistivity was in the order of 10^{14} Ω × m and 10^{15} Ω × m when measured under 2 kV/mm, and between 10^{13} Ω × m and 10^{15} Ω × m when measured under 30 kV/mm.

3.2. Dielectric Spectroscopy

The dielectric properties were measured in the range of 10^{5} to 10^{-1} Hz. However, only three frequency values were deeply investigated, corresponding to frequency domains where different behaviors with respect to dielectric losses were observed during the initial characterization of the material [22]: 10^{4} Hz, 10^{2} Hz and 10^{-1} Hz, corresponding to high, medium and low frequency, respectively. Results of electrical capacitance and dielectric loss factor (tan δ), measured for ageing tests under 60 kV/mm and 30 kV/mm at 70, 80 and 90 °C and at 10^{4}, 10^{2} and 10^{-1}, as a function of ageing time were presented in [23]. In this section, we present only results for ageing tests under 30 kV/mm and 60 kV/mm at 90 °C and 10^{2} Hz, as a function of ageing time (Figures 5 and 6).

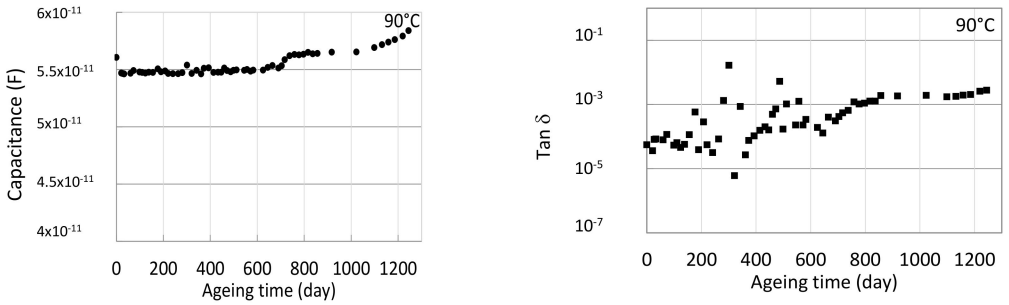


Figure 5. (**a**) Capacitance, (**b**) tan δ measured at 10^{2} Hz on samples aged at 90 °C and 30 kV/mm.

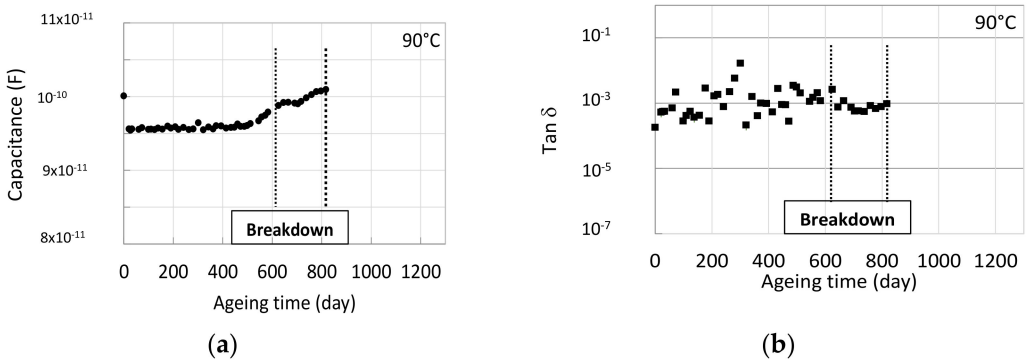


Figure 6. (**a**) Capacitance, (**b**) tan δ measured at 10^{2} Hz on samples aged at 90 °C and 60 kV/mm.

Tan δ measurements did not show any significant variation with ageing time for all ageing test conditions except for 90 °C and 30 kV/mm, where an increase of tan δ was observed at 10^2 Hz after 600 days of the ageing test. This increase could be linked to the semicon-insulation interface. It has been reported that above 10^2 Hz, the dielectric behavior of the XLPE is dominated by the series resistance of the semicon layers [24]. An increase of electrical capacitance was observed at 90 °C after about 700 days under 30 kV/mm and after 400 days under 60 kV/mm. In addition, two dielectric breakdowns occurred under 90 °C and 60 kV/mm after 625 days and 817 days of ageing test. For ageing at 70 °C and 80 °C, and for both applied electric fields, the electrical capacitance did not show any significant variation.

3.3. Space Charge

In this section, we present only results of space charge density and internal electric field (generated by space charge injected at the electrodes or coming from the material itself) for samples aged at 90 °C under 30 kV/mm and for samples aged at 90 °C under 60 kV/mm.

Results of charge density distributions at 90 °C under 30 kV/mm (Figure 7) show an inversion of the dominant type of charge at the electrodes from homocharge to heterocharge after 156 days. Then, dominant the heterocharge increased. The increase of heterocharge could mean that the conduction phenomenon is dominant compared to injection. This increase was followed by a decrease and a stabilization of heterocharge, for this ageing test.

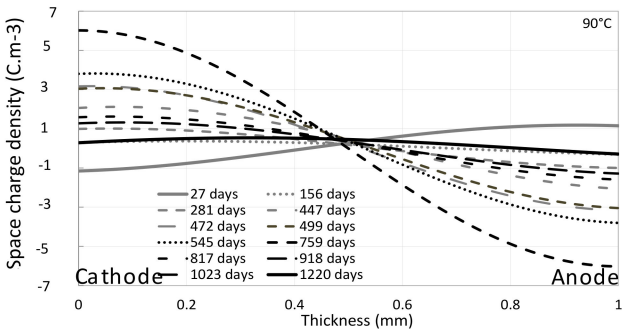


Figure 7. Space charge density evolution for samples aged under 30 kV/mm at 90 °C.

The evolution of the residual electric for ageing at 90 °C under 30 kV/mm (Figure 8) shows an inversion followed by an increase. The internal electric field reached a maximum of 200% of the applied field. This suggests distortion of the electric field due to space charge effects. The residual electric field decreased then tended to stabilize. In the same manner, analysis of space charge density at 90 °C under 60 kV/mm showed a change from dominant homocharge to dominant heterocharge near the electrodes after 447 days (Figure 9). Then, an increase followed by a decrease of heterocharge appeared. Residual electric field evolutions for ageing at 90 °C under 60 kV/mm are presented in Figure 10 and show that after an electric field inversion, an increase is observed, followed by a decrease after 817 days. For this ageing test, the results were not presented after 817 days because of the dielectric breakdown of all samples, except one. This remaining sample was kept for physical and chemical characterizations. It is important to note that most of the samples that underwent under breakdown had copper ions. The levels of residual electric field reached a maximum value of 55 kV/mm at 90 °C which represents about 92% of the applied field. Changes observed in the electrical field correlated with space charge density evolution. To conclude, the evolution of space charge density and of the electric field appeared faster for the lowest applied electric field.

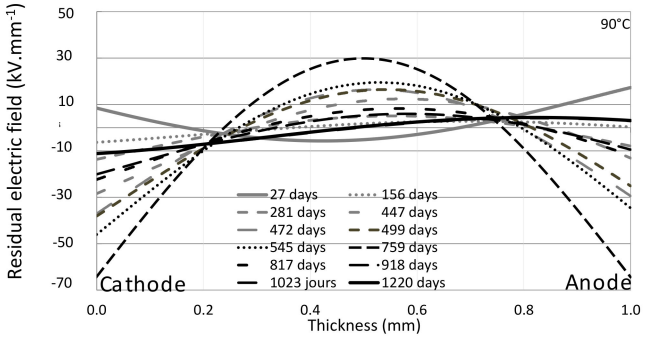


Figure 8. Residual electric field evolution for samples aged under 30 kV/mm at 90 °C.

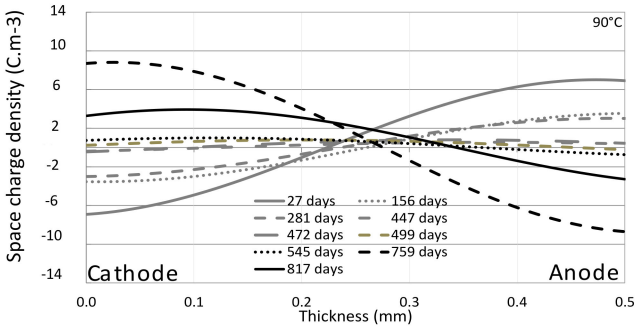


Figure 9. Space charge density evolution for samples aged under 60 kV/mm at 90 °C.

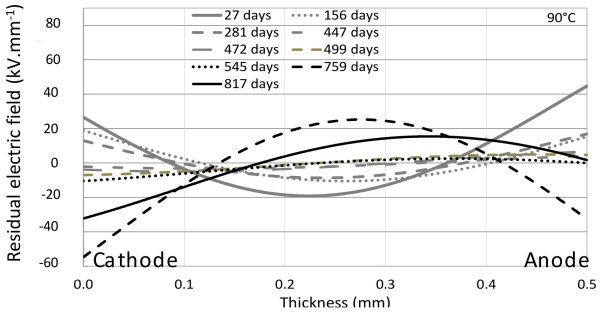


Figure 10. Residual electric field evolution for samples aged under 60 kV/mm at 90 °C.

When analyzing the internal electric field and charge density evolution, three main periods corresponding to different space charge and electric field behaviors were found:

- Period 1: Change from dominant homocharge to dominant heterocharge and inversion of the residual electric field.
- Period 2: Increase in dominant heterocharge and in residual electric field.
- Period 3: Decrease in space charge density and residual electric field, followed by a possible stabilization.

At this stage of the ageing test, the three periods appeared for ageing at 90 °C under 30 and 60 kV/mm, while only the two first periods appeared at 70 and 80 °C.

Finally, it must be noted that electrical breakdown occurred for eight out of the nine samples aged at 90 °C and 60 kV/mm. These breakdowns occurred after different ageing times and for samples used for different electrical characterization. To try to understand the reason for breakdowns some analyses were performed.

To try to understand the different observed phenomena, an ageing model based on the results obtained at 90 °C was proposed.

4. Ageing Kinetics

As stated above, one of the main objectives of this work was to understand the electrical behavior of the material when it is subjected to thermal and electrical DC stresses. We propose an ageing model and hypotheses based on the electrical results obtained for the Rogowski samples, especially those obtained at 90 °C.

4.1. Hypotheses

As no systematic physical and chemical characterization of the material (such as carbonyl index, melting point, etc.) was done in parallel with electrical measurements during ageing, hypotheses can only be used to try to explain the different observed phenomena. The working hypotheses for this paper concern the displacement of charge carriers, i.e., any polar molecules present in the insulation and antioxidant(s) reaction in the insulation material. For instance, antioxidant(s), which are often polar molecules, are added to the insulation during manufacture in order to prevent oxidation. Due to the experimental set-up with Rogowski plaques aged in an oven with air, it seems reasonable to assume that water and oxygen from the air can diffuse in the sample and thus the antioxidant(s) react to protect the insulation material. Such an antioxidant(s) and antioxidant(s) reaction could have an impact on the development of space charge.

4.2. Stage 0: Uniform Polarization at the Initial State

The material is considered at its steady state and thus charge carriers are likely to be uniformly distributed in the bulk of the material. The application of a low electric field to the material can lead to a uniform polarization within the insulation thickness. It must be pointed out that the TSM is only sensitive to the average value of the charge in a plane parallel to the electrodes. As the distribution of charge carriers is homogeneous, and because of the compensation of electrical contribution of the charge carrier at each plane, the total charge compensation in a plane gives a zero TSM signal. Thus, electrical charges due to polarization of charges carries such as antioxidant(s) cannot be detected by this method. Figure 11 shows a schematic view of the charges compensation in a plane resulting from the polarization of polar molecules.

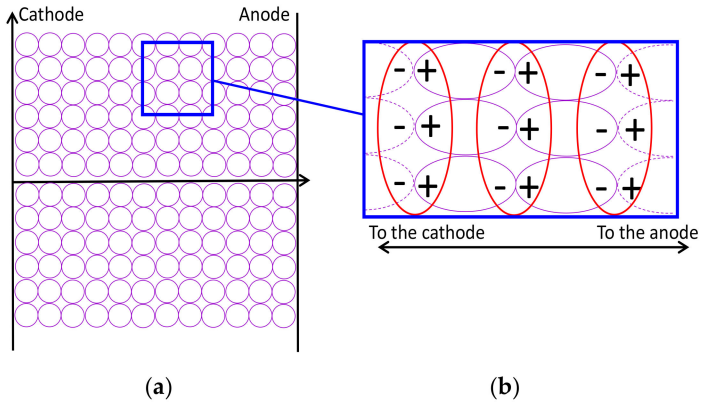


Figure 11. (**a**) Uniform distribution of charge carriers, such as antioxidants, in the thickness; (**b**) compensation of charge on a plane parallel to the electrodes.

4.3. Stage 1: Establishement of Dominant Homocharge

When a high electric field is applied, charge injected at the electrodes become dominant compared to intrinsic carriers initially present in the insulation material. The study of conduction mechanisms of XLPE at the initial state [22] showed that, whatever the temperature and the electric field, the DC conduction properties were mainly controlled by an interface injection-controlled mechanism (Schottky) [22], leading to the accumulation of space charge near the electrodes.

Space charge data showed that homocharges were dominant at the beginning of each ageing condition, which indicates that charge injection was dominant compared to conduction. We can also assume that the distribution of charge carriers remained uniform at this stage and only injected charges localized near electrodes were detected by the TSM. Charges injected near the electrodes led to an image charge effect which resulted in a reduced energy barrier (Figure 12) [23]. The increase of the applied electric field coupled with the presence of charge image made charge injection easier and consequently resulted in an increase of space charge amount within the insulating material.

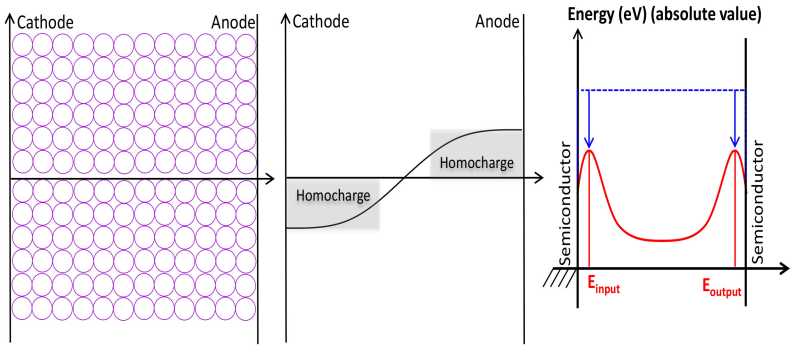


Figure 12. (**a**) Uniform distribution of the polarized charge carriers such as antioxidants; (**b**) dominant homocharge; (**c**) effect of injected charges and applied field on the energy barriers.

4.4. Stage 2: Development of the Heterocharge and Decrease of Apparent Homocharge

In this step, we consider that the mechanism of charge injection is still present and as the sample studied is in an atmospheric environment, we assume that oxygen begins to diffuse, and antioxidant(s) starts to react (Figure 13a). Due to the geometry of the sample studied, this would mainly occur near the electrodes. Consequently, a concentration gradient of charge carriers could appear which would lead to the polarization gradient seen in space charge measurements. This suggests the formation of heterocharges near electrodes, and a progressive decrease of homocharge levels that, however, remains dominant compared to heterocharges (Figure 13b).

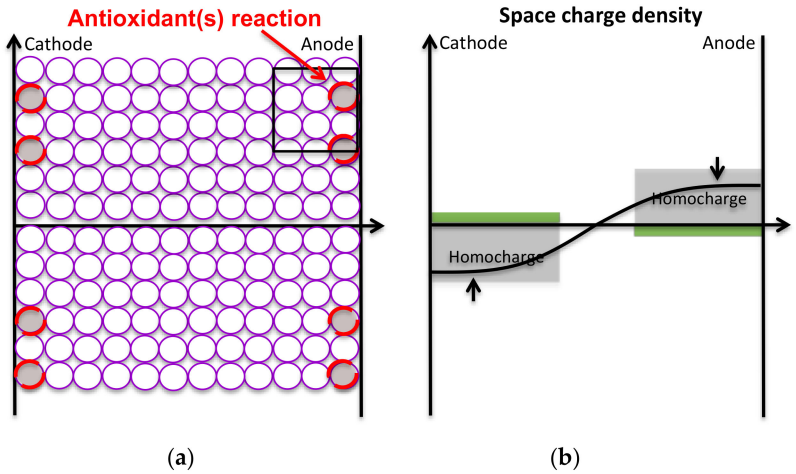


Figure 13. (**a**) Antioxidant(s) reaction near the electrodes; (**b**) appearance of a minority heterocharge due to the polarization gradient (**b**) (black inset).

4.5. Stage 3: Apparent Compensation of Homocharge and Heterocharge

At this step, the injection phenomenon is still present as the oxygen continues to diffuse and the antioxidant(s) to react (Figure 14a). The concentration gradient of charge

carriers leads to the increase of heterocharge until the perfect compensation of the two types of space charge (Figure 14b). At this stage, although both types of charges are present, the detected space charge density is quasi-zero.

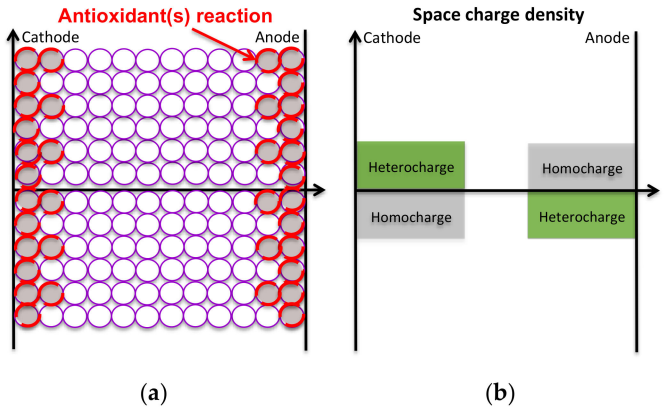


Figure 14. (**a**) Antioxidant(s) reaction near the electrodes; (**b**) apparent compensation of homocharge and heterocharge.

4.6. Stage 4: Establishment of Dominant Heterocharge

During this stage, the injection phenomenon, represented by the presence of homocharges, plus the antioxidant(s) reaction phenomenon, continue leading to the presence of a dominant heterocharge in the material. This charge attracts those present at the electrode. Energy barriers decrease and the charge injection at the electrodes becomes easier (Figure 15). Some injected charges, which could not be trapped near the electrodes, could migrate towards the opposite electrode by conduction mechanism and form heterocharges. These charges would be added to the heterocharge resulting from the antioxidant(s) reaction. Simultaneously, homocharge tends to accumulate at the electrode because of easier injection at the contact. At this step, since the increase of heterocharge is limited by the increase of homocharge, heterocharge seems to remain dominant. When equilibrium is established between injection and conduction, the heterocharge tends to stabilize.

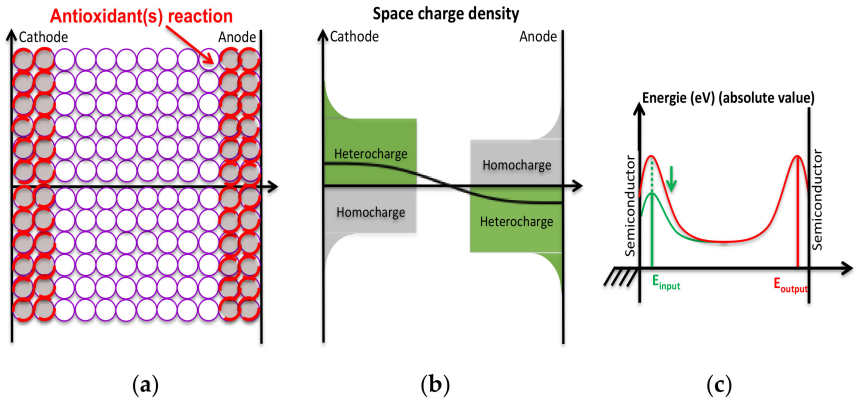


Figure 15. (**a**) Antioxidant(s) reaction near the electrodes; (**b**) space charge distribution with enhancement of homocharges at the electrodes; (**c**) effect of heterocharges on the input and output energy barrier.

4.7. Stage 5: Increase of the Heterocharge

At this step, space charge density is characterized by an increase of the dominant heterocharge, due to the further antioxidant(s) reaction (combined effect of concentration gradient of polar species and accumulation of injected charges moving towards the opposite electrodes). This implies a modification of injection/conduction equilibrium. A conduction mechanism is dominant at this stage of ageing. Even if the homocharge increases, lowering

the energy barrier at contact, its decrease seems to be lower compared to the heterocharge. This can be explained by a reduction of input and output energies (Figure 16). Moreover, some injected charges can lose a part of their energy when crossing through the insulation, which limits their ejection and thus increases the accumulation of heterocharge.

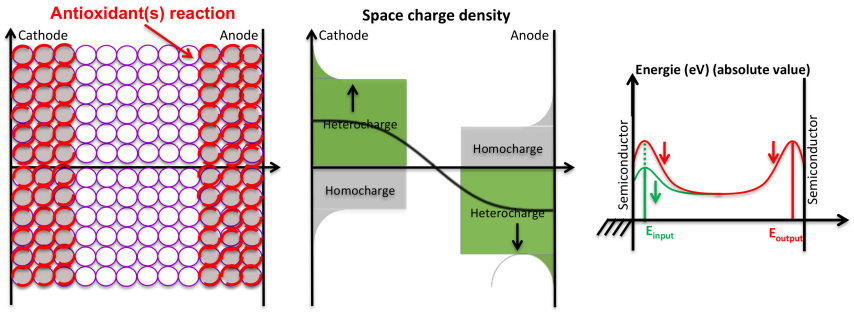


Figure 16. (**a**) Antioxidant(s) reaction near the electrodes; (**b**) increase of the heterocharge; (**c**) decrease of input and output energy barriers.

4.8. Stage 6: Localized Oxidation of XLPE

At this stage, we propose that most of the antioxidant(s) has reacted and the probability of oxidizing the polymer chain, and subsequently the formation of carbonyl groups, has increased. In our study, an increase of the electrical capacitance and/or loss factor, which indicates an increase of the complex permittivity, was observed after various ageing time for the sample aged at 90 °C. This increase could be an indication of the oxidation phenomena occurring in the material [25]. At this step, we assume that the polarization gradient becomes less significant and so its contribution to the heterocharge can be negligible. During ageing, the antioxidant(s) reaction is essentially localized very close to the electrodes. It contributes, in particular, to the trapping of injected charges. The polar species resulting from XLPE oxidation also contributes to heterocharge formation, especially concerning species containing carbonyl functions (Figure 17).

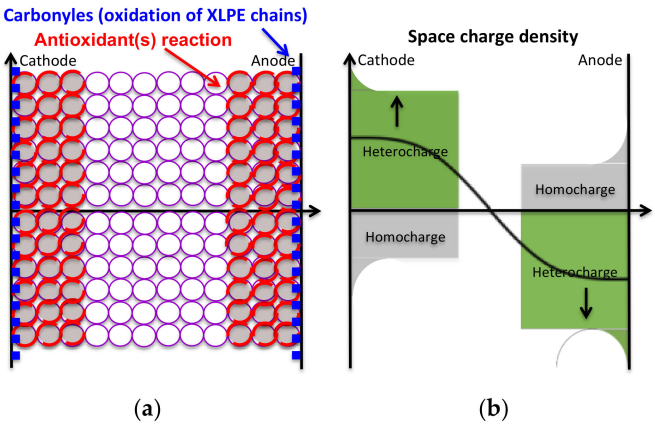


Figure 17. (**a**) Maximum level of dominant heterocharge; (**b**) beginning of the oxidation of XLPE chains at the electrodes.

4.9. Stage 7: Oxidized XLPE Layer

At this final stage, we propose that the increase of the XLPE oxidized layer is limited by the depth diffusion of the oxygen in the material. If the existence of such a layer is taken into account, the generation of heterocharge should slow down and then stop, since the access of the oxidizing agent to reactive polymer chains becomes more difficult. To this effect will probably be added the progressive loss of the insulating property of the oxidized

layer, which could result in decreasing the effective insulation thickness withstanding the applied electric field.

Under these conditions of electrical stress, the heterocharge remains stable but the lowering of the energy barrier at the contact facilitates the injection, and thus the establishment, of homocharge.

The compensation phenomenon associated with the polarization gradient, and the progressive accumulation of charge carriers at the electrode, no longer exists. Therefore, under these conditions, the input and output energy barriers increase (Figure 18). This leads to a possible decrease of the space charge density produced by both a stabilized heterocharge and an increase in homocharge.

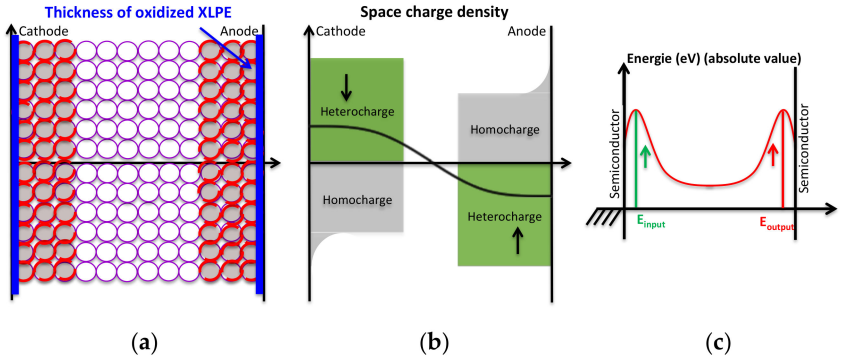


Figure 18. (**a**) End of the increase of the oxidized XLPE layer; (**b**) decrease of dominant heterocharge; (**c**) increase of input and output energy barriers.

The same ageing stages were observed for all the ageing tests, regardless of the thickness of the samples. However, different kinetics, as a function of the temperature and the insulation thickness were observed. As mentioned, no systematic physico-chemical analysis such as Fourier Transform Infrared Spectroscopy (FTIR) and Differential Scanning Calorimetry (DSC) was performed during the ageing. The few analyses done by Borealis are summarized in Table 1.

Table 1. Summary of physico-chemical analyses and capacitance results.

Sample	Applied Field	Capacitance Evolution	Carbonyl Index	Tmelting (°C)	Crystallinity (%)
Reference	0	Not followed	0.5	104	40
Aged at 90 °C	60 (broken)	↗ 400 days	1.5	104	32
	60	↗ 400 days	1	104	36
	30	↗ 700 days	0.8	104	39

The carbonyl index was calculated with FTIR spectroscopy at a different location of the XLPE under the semicon electrode [26] as shown in Figure 19.

Temperature melting and crystallinity were measured by DSC.

Measurements carried out at 90 °C and 60 kV/mm were done on two samples (dielectric breakdown occurred after 837 days of ageing on one sample). Results were compared with a "reference" virgin sample (no applied stresses).

An increase of carbonyl index was observed for samples where an apparent increase of electrical capacitance was seen. It should also be noticed that one sample aged at 90 °C and 60 kV/mm, having experienced a breakdown, was contaminated with copper ions; and the presence of metal ions can have accelerated the oxidation. No significant evolution was observed in the melting temperature and in the crystallization rate of the material for all samples.

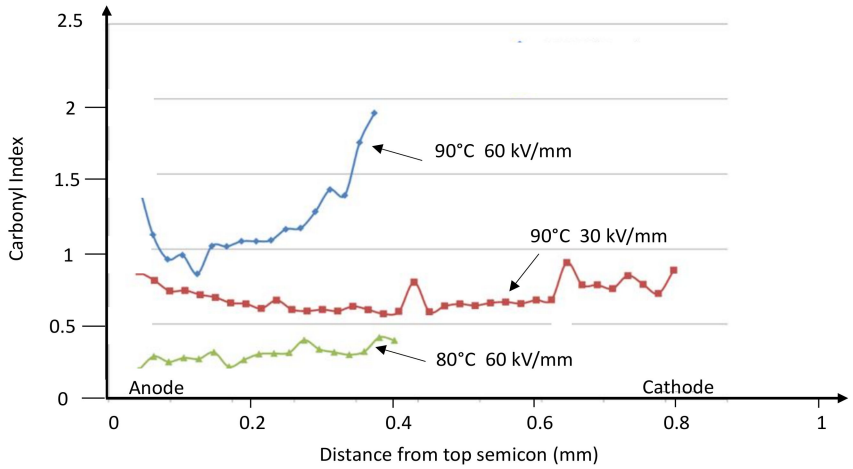


Figure 19. Distribution of carbonyl index as a function of insulation thickness for ageing carried out at 90 °C and 80 °C after 837 days of ageing.

Finally, the distribution of carbonyl index as a function of the thickness for different stress levels was performed by FTIR on three samples (one aged under 90 °C-60 kV/mm, a second subjected to 90 °C-30 kV/mm and a third aged under 80 °C-60 kV/mm) after 837 days of ageing. Results are given in Figure 18. The highest levels of carbonyl index were exhibited by the samples submitted to the highest stresses i.e., 60 kV/mm and 90 °C. These higher levels located near electrodes were also measured on a sample aged under 30 kV/mm at 90 °C. This seems to support the hypothesis about the antioxidant(s) reaction near the electrodes. In some of these samples we found traces of copper. To make our assumptions more reliable, it would be necessary to replicate these measurements on a larger number of samples. This hypothesis should also be verified with systematic analysis of carbonyl index.

No localized increase was observed on sample aged at 80 °C, which confirms that the observed effects during ageing test were mainly due to the temperature.

5. Conclusions

The aim of the present work was to understand the influence of electrical and thermal stress on conventional HVDC XLPE cable insulation material qualified for voltages up to 320 kV, in order to verify the properties of the insulation system when used for a long time under HVDC. Ageing tests were performed for 1220 days in air on Rogowski XLPE samples submitted to DC electric fields of 30 kV/mm and 60 kV/mm, at temperatures of 70, 80 and 90 °C. Selected electrical properties, such as capacitance, tan δ, volume resistivity and space charge accumulation were followed during these ageing tests, in order to identify potential ageing markers and propose a lifetime model by using these ageing markers.

It is important to note that all the potential ageing markers, selected at the beginning of this study, did not show significant evolution during the ageing tests. In particular, the volume resistivity, which is a key electrical property of HVDC materials, remained constant for all ageing conditions studied.

Analysis of the dielectric spectra has shown an increase of the capacitance for ageing at 90 °C after about 700 days under 30 kV/mm, and after 400 days under 60 kV/mm. This increase of the capacitance might be linked to the formation of carbonyl groups. Tan δ increased for ageing under 90 °C-30 kV/mm but did not show any variation for the other ageing conditions.

Space charge variation with time appeared sensitive to the ageing conditions and thus could be considered as a possible ageing marker. Analysis of space charge accumulation in the insulation material showed the same evolution for all ageing conditions but with different kinetics during ageing. For the same ageing temperature, the different ageing stages appeared faster for the lowest electric field (30 kV/mm vs. 60 kV/mm).

Moreover, the long-term ageing tests allowed observation of a succession of different periods with respect to the space charge behavior, depending on injection/conduction properties. This kinetic was initially controlled by dominant homocharges at the electrodes, and then, depending on ageing time, they became a heterocharges. After a period of stabilization, an increase of heterocharge was observed up to a maximum value, and then heterocharge decreased.

Author Contributions: Data curation, S.A., W.F., C.M., P.H., D.l.R., V.E. and C.J.A.; Formal analysis, A.H.; Writing—review & editing, H.Y. and J.C. All authors have read and agreed to the published version of the manuscript.

Funding: This research received no external funding.

Institutional Review Board Statement: Not applicable.

Informed Consent Statement: Not applicable.

Data Availability Statement: The data presented in this study are available on request from the corresponding author.

Conflicts of Interest: The authors declare no conflict of interest.

References

1. Mazzanti, G.; Marzinotto, M. *Extruded Cables for High-Voltage Direct-Current Transmission: Advances in Research and Development*; IEEE Press Series on Power Engineering; Wiley-IEEE Press: Hoboken, NJ, USA, 2013.
2. Fothergill, J.C. The coming of Age of HVDC extruded power cables. In Proceedings of the 2014 IEEE Electrical Insulation Conference (EIC), Philadelphia, PA, USA, 8–11 June 2014; pp. 124–137.
3. Mazzanti, G.; Marzinotto, M. Relationship between the expressions for electrical resistivity and the field profiles in HVDC cable insulation. In Proceedings of the 2016 IEEE Conference on Electrical Insulation and Dielectric Phenomena (CEIDP), Toronto, ON, Canada, 16–19 October 2016; pp. 947–950.
4. Zhou, Y.; Peng, S.; Hu, J.; He, J. Polymeric insulation materials for HVDC cables: Development, challenges and future per-spective. *IEEE Trans. Dielectr. Electr. Insul.* **2017**, *24*, 1308–1318. [CrossRef]
5. Castellon, J.; Agnel, S.; Notingher, P. Review of space charge measurements in high voltage DC extruded cables by the thermal step method. *IEEE Electr. Insul. Mag.* **2017**, *33*, 34–41. [CrossRef]
6. Montanari, G.C. Bringing an insulation to failure: The role of space charge. *IEEE Trans. Dielectr. Electr. Insul.* **2011**, *18*, 339–364. [CrossRef]
7. Wang, X.; Liu, Q.; Zhang, X.; Wu, K.; Zhang, C.; Li, W. Study on space charge behavior of XLPE after long-term aging un-der temperature gradient and DC stress. In Proceedings of the 2016 International Conference on Condition Monitoring and Diagnosis (CMD), Xi'an, China, 25–28 September 2016; pp. 741–744.
8. Chen, G.; Hao, M.; Xu, Z.; Vaughan, A.; Cao, J.; Wang, H. Review of high voltage direct current cables. *CSEE J. Power Energy Syst.* **2015**, *1*, 9–21. [CrossRef]
9. Fu, M.; Hou, S.; Lui, T.; Lv, Z.; Wu, K.; Wang, Y.; Wang, X. Mechanism of space charge accumulation in crosslinked polyethylene under temperature gradient. In Proceedings of the 2015 IEEE 11th International Conference on the Properties and Applications of Dielectric Materials (ICPADM), Sydney, NSW, Australia, 19–22 July 2015; pp. 356–359.
10. Mazzanti, G. Issues and Challenges for HVDC Extruded Cable Systems. *Energies* **2021**, *14*, 4504. [CrossRef]
11. Abou-Dakka, M.; Bulinski, A.; Bamji, S.S. Effect of additives on the performance of cross-linked polyethylene subjected to long term single and periodically reversed polarity DC voltage. *IEEE Trans. Dielectr. Electr. Insul.* **2013**, *20*, 654–663. [CrossRef]
12. Tefferi, M.; Li, Z.; Cao, Y.; Uehara, H.; Chen, Q. Novel EPR-Insulated DC Cables for Future Multi-Terminal MVDC Integration, IEEE Electr. *Insul. Mag.* **2019**, *35*, 20–27. [CrossRef]
13. Hayashi, N.; Suzuki, H.; Miyake, H.; Tanaka, Y.; Maeno, T. Effect of cumylalcohol in XLPE on space charge formation and electric breakdown under DC high electric field. In Proceedings of the 2011 Annual Report Conference on Electrical Insulation and Dielectric Phenomena, Cancun, Mexico, 16–19 October 2011; pp. 145–148. [CrossRef]
14. Dissado, L.; Laurent, C.; Montanari, G.; Morshuis, P. Demonstrating a threshold for trapped space charge accumulation in solid dielectrics under dc field. *IEEE Trans. Dielectr. Electr. Insul.* **2005**, *12*, 612–620. [CrossRef]
15. Boyer, L.; Mirebeau, P.; Vershnin, K.; Tzimas, A.; Castellon, J.; Notingher, P. Follow up of space charge distributions in HVDC cable during a Pre-Qualification test using the Pulse Electroacoustic technique and the Thermal Step Method. In Proceedings of the 10th International Conference on Insulated Power Cables, Versailles, France, 23–27 June 2019.
16. Fukuma, M.; Tomita, H.; Maeno, T. Space charge measurement for 27mm thick XLPE sample in PEA method. In Proceedings of the 2014 International Symposium on Electrical Insulating Materials, Niigata, Japan, 1–5 June 2014; pp. 89–92.

17. Haque, N.; Dalai, S.; Chakravorti, S.; Chatterjee, B. Space charge measurement in dielectrics using Pressure Wave Propagation method. In Proceedings of the 2015 International Conference on Condition Assessment Techniques in Electrical Systems, Bangalore, India, 10–12 December 2015; pp. 226–230.
18. Ala, G.; Caruso, M.; Cecconi, V.; Ganci, S.; Imburgia, A.; Miceli, R.; Romano, P.; Viola, F. Review of acoustic methods for space charge measurement. In Proceedings of the 2015 AEIT International Annual Conference (AEIT), Naples, Italy, 14–16 October 2015; pp. 1–6.
19. Seguchi, T.; Tamura, K.; Ohshima, T.; Shimada, A.; Kudoh, H. Degradation mechanisms of cable insulation materials during radiation–thermal ageing in radiation environment. *Radiat. Phys. Chem* **2011**, *80*, 268–273. [CrossRef]
20. Eriksson, V.; Andersson, J.; Englund, V.; Hagstrand, P.; Kontro, A.; Nilsson, U.H.; Silfverberg, E.; Smedberg, A. Long term performance of XLPE insulation materials for HVDC cables. In Proceedings of the Conference Jicable'15, Versailles, France, 21–25 June 2015.
21. Cenes, J.; Teyssedre, G.; le Roy, S.; Berquez, L.; Hondaa, P.; Eriksson, V.; Loyens, W. Assessment of Ageing in the Insulation of HVDC Model Cables under Thermo-electric Stress. In Proceedings of the 2nd International Conference on Dielectrics (ICD), Budapest, Hungary, 1–5 July 2018.
22. Hascoat, A.; Castellon, J.; Agnel, S.; Frelin, W.; Egrot, P.; Hondaa, P.; Ammi, S.; Le Roux, D. Study and analysis of conduction mechanisms and space charge accumulation phenomena under high applied DC electric field in XLPE for HVDC cable application. In Proceedings of the 2014 IEEE Conference on Electrical Insulation and Dielectric Phenomena (CEIDP), Des Moines, IA, USA, 19–22 October 2014; pp. 530–533.
23. Hascoat, A. Etude et Modélisation du Vieillissement sous Contraintes Électrothermiques de L' isolant pour Câble de Transport d'Énergie Haute Tension à Courant Continu. Ph.D. Thesis, Université de Montpellier, Montpellier, France, 2016.
24. Fothergill, J.C.; Dodd, S.; Dissado, L.; Liu, T.; Nilsson, U.H. The measurement of very low conductivity and dielectric loss in XLPE cables: A possible method to detect degradation due to thermal aging. *IEEE Trans. Dielectr. Electr. Insul.* **2011**, *18*, 1544–1553. [CrossRef]
25. Vandbakk, M. Organic Contaminations in Sub-Marine AC and DC High-Voltage Cables. Ph.D. Thesis, Norwegian University of Science and Technology, Trondheim, Norway, 2012.
26. Wang, Y.; Wu, J.; Yi, S.; Yin, Y. Research on simultaneous measurement of space charge and conduction current for ther-mally aged cross-linked polyethylene. In Proceedings of the 2017 1st International Conference on Electrical Materials and Power Equipment (ICEMPE), Xi'an, China, 14–17 May 2017; pp. 383–387.